



**QUEEN'S
UNIVERSITY
BELFAST**

Review of frequency stability services for grid balancing with wind generation

Boyle, J., Littler, T., & Foley, A. (2018). Review of frequency stability services for grid balancing with wind generation. *IET The Journal of Engineering*, 1-5. <https://doi.org/10.1049/joe.2018.0276>

Published in:
IET The Journal of Engineering

Document Version:
Publisher's PDF, also known as Version of record

Queen's University Belfast - Research Portal:
[Link to publication record in Queen's University Belfast Research Portal](#)

Publisher rights

Copyright 2018 the authors.

This is an open access article published under a Creative Commons Attribution License (<https://creativecommons.org/licenses/by/4.0/>), which permits unrestricted use, distribution and reproduction in any medium, provided the author and source are cited.

General rights

Copyright for the publications made accessible via the Queen's University Belfast Research Portal is retained by the author(s) and / or other copyright owners and it is a condition of accessing these publications that users recognise and abide by the legal requirements associated with these rights.

Take down policy

The Research Portal is Queen's institutional repository that provides access to Queen's research output. Every effort has been made to ensure that content in the Research Portal does not infringe any person's rights, or applicable UK laws. If you discover content in the Research Portal that you believe breaches copyright or violates any law, please contact openaccess@qub.ac.uk.

Review of frequency stability services for grid balancing with wind generation

eISSN 2051-3305

Received on 4th May 2018

Accepted on 11th June 2018

doi: 10.1049/joe.2018.0276

www.ietdl.org

James Boyle¹ ✉, Timothy Littler¹, Aoife Foley²¹School of Electronics, Electrical Engineering and Computer Science, Queen's University Belfast, Belfast, Northern Ireland²School of Mechanical and Aerospace Engineering, Queen's University Belfast, Belfast, Northern Ireland

✉ E-mail: jboyle27@qub.ac.uk

Abstract: Frequency stability in power systems is achieved by active power control, which aims to balance grid generation with load demand. Historically, grid balancing services have been provided by synchronous thermal generating units. As wind penetration levels increase on the power system, it is essential that wind turbine generators (WTGs) provide robust, reliable frequency stability services to grid operators. Like other forms of renewable generation such as solar photovoltaic generation, modern variable speed WTGs are connected to the power system using power electronic converters. This non-synchronous connection decouples the natural inertia of the WTG from the grid frequency. As system non-synchronous penetration levels increase, non-synchronous generation will be required to participate in frequency stability services such as automatic generation control. This study presents a review of WTG frequency response systems that allow WTGs to participate in frequency stability services by emulating the natural inertia and droop characteristics of conventional synchronous thermal generators. Power system simulations performed in MATLAB/Simulink show that the addition of emulated inertia and droop controllers into WTG's power/speed control systems can reduce the rate of change of frequency and increase frequency nadir when the power system is subject to a load/generation imbalance.

1 Introduction

As variable renewable generation levels grow to significant penetrations on the all-Ireland power system, grid operators will struggle to maintain system stability and reliability by depending solely on synchronous thermal generators to provide grid balancing services. Renewable generation such as wind can also offer reliable ancillary services to grid operators. In power systems, stability and reliability are maintained by managing system inertia and frequency response during normal operating conditions and disturbances. In conventional power systems, employing synchronous thermal generators, the initial rate of change of frequency (RoCoF) of small signal frequency disturbances is naturally retarded by an increase/decrease in power generation, due to the natural inertia of the large rotating masses of committed generating units [1]. This natural inertial response occurs due to *stiff* coupling between the synchronous generator and the grid frequency. State-of-the-art variable speed wind turbine generators (VSWTGs) are, however, either partially or fully decoupled from the grid frequency by power electronic converters. This decoupling means that VSWTGs provide little or no natural inertial response to grid imbalances; a response that is essential for maintaining frequency stability [2]. In addition to the inertial response of conventional generating units, primary and secondary responses are required to balance generation with load demand, thereby restoring system frequency to its nominal value. Currently, primary and secondary operating reserves are used in Ireland and the UK such as many other countries, to provide these responses, using governor droop characteristics and spinning reserve, respectively. Traditionally these automatic generation control (AGC) services are provided by synchronous thermal generators such as coal, peat, natural gas, and oil. If WTGs were also permitted to offer AGC services such as conventional synchronous generators, then grid operators would have access to additional resources when needed. However, to arrange this for grid operation, the robustness of AGC from variable renewable generation must be analysed. Therefore, wind farm operators need to examine, develop, and test that their power electronic converters can provide AGC to comply with appropriate grid code standards. This paper presents a review of WTG frequency response systems that allow WTGs to participate in grid balancing, AGC services by emulating the natural inertia

and droop characteristics of conventional synchronous thermal generators.

2 Frequency response systems

Unlike conventional synchronous generators, modern VSWTGs are either partially (Type C WTGs) or fully decoupled (Type D WTGs) from the grid frequency by power electronic converters [3]. This decoupling means that VSWTGs provide little or no natural active power response to frequency events. Active power controllers can be used to adjust the VSWTG's power electronic converter's active power reference to increase or decrease generation in response to frequency events [4, 5]. A frequency response scheme that mimics the inertia and droop characteristics of a synchronous generator is proposed in [4]. The control scheme releases the *hidden* inertia of the VSWTG by providing an active power response that is activated by RoCoF and frequency deviation. This would allow VSWTGs to participate in frequency control schemes, by providing synthetic inertial responses such as that of conventional synchronous generators, which have stiff coupling to the grid frequency. The hidden inertia of VSWTGs can be released in many ways. A novel control strategy that shifts the WTG's maximum power point tracking (MPPT) curve to virtual inertia control curves according to frequency deviations is proposed and investigated in [6]. Fixed frequency responses to frequency events are investigated in [7], while Kang *et al.* [8] propose a stable adaptive inertial control scheme. Although frequency response strategies differ in the literature surveyed, the objective of all schemes is to release the kinetic energy of the turbine and generator to provide grid balancing, AGC services. A frequency response system based on the emulated inertia and droop controller proposed in [4] was investigated using a simplified power system model built using MATLAB/Simulink.

3 Modelling

3.1 WT model

A wind farm was modelled using an aggregate model of a WT doubly fed induction generator (DFIG), where one large DFIG was used to represent the entire wind farm. This is a proven modelling

technique for power system stability studies [9]. The mechanical power output of the WT is given by the equation below:

$$P_m = \frac{1}{2} C_p(\lambda, \beta) \rho A v^3 \quad (1)$$

where P_m , C_p , ρ , A , v , λ , β are the mechanical output power, power coefficient, air density, turbine blade swept area, wind speed, tip speed ratio, and blade pitch angle. Equation (2) is used to model the power coefficient of the WT [10]

$$C_p(\lambda, \beta) = c_1 \left(\frac{c_2}{\lambda_i} - c_3 \beta - c_4 \right) e^{c_5/\lambda_i} + c_6 \lambda \quad (2)$$

where

$$\lambda_i = \left(\frac{1}{\lambda + 0.08\beta} - \frac{0.035}{\beta^3 + 1} \right)^{-1} \quad (3)$$

The coefficients used in (2) to model the turbine power coefficient characteristic are $c_1 = 0.5176$, $c_2 = 116$, $c_3 = 0.4$, $c_4 = 5$, $c_5 = 21$, and $c_6 = 0.0068$ [10]. The maximum value of $C_p = 0.48$ is achieved with a blade pitch angle of 0° and a nominal tip speed ratio of 8.1.

3.1.1 Power/speed control: Power/speed control is achieved in the WTG model by controlling the quadrature component of the current injected into the DFIG's rotor windings by the rotor-side converter [11]. Manipulating the magnitude of the quadrature component of the rotor current I_{qr} controls the active power output of the DFIG. The rotor speed ω_r is measured and used to determine the optimal active power reference P_{ref} , which is determined by a predefined MPPT characteristic. The actual electrical power output P_{elec} is measured and added to the calculated power loss P_{loss} . The sum of P_{elec} and P_{loss} is then subtracted from P_{ref} to produce an error signal P_{error} . This error signal is then passed through a proportional plus integral controller to produce the rotor current quadrature component reference signal I_{qr}^* .

3.2 Operating zones

WTGs operate in four distinct zones as illustrated in Fig. 1.

The expression used to determine the power/speed controller's active power reference differs for each operating zone. The four operating zones will be discussed in the following sections.

3.2.1 Zone 1: cut-in zone: For very low wind speeds, the WTG's active power reference is zero; hence, no active power is supplied to the grid. When the rotor speed reaches the cut-in speed (point A in Fig. 1), the WTG operates at quasi-constant speed until the mechanical power generated reaches point B. When operating in the cut-in zone, ($\omega_A < \omega_r \leq \omega_B$), the active power reference is given by the equation below:

$$P_{ref} = \frac{K_{opt} \omega_B^3}{(\omega_B - \omega_A)} (\omega_r - \omega_A) \quad (4)$$

3.2.2 Zone 2: MPPT zone: In the operating zones B and C, maximum power is extracted from the available wind resource. It can be noted that the curves B and C intersects the maxima of the turbine power curves for all wind speeds between 7 and 12 m/s. When operating in the MPPT zone, the active power reference is a cubic function of rotor speed ω_r as shown in (5). The constant K_{opt} is determined by the turbine P - ω characteristic

$$P_{ref} = K_{opt} \omega_r^3 \quad (5)$$

3.2.3 Zone 3: quasi-constant speed zone: In the operating zones C and D, the WTG operates at quasi-constant speed until the mechanical power generated reaches the WTG's maximum active power rating P_{max} (point D). When operating in the quasi-constant

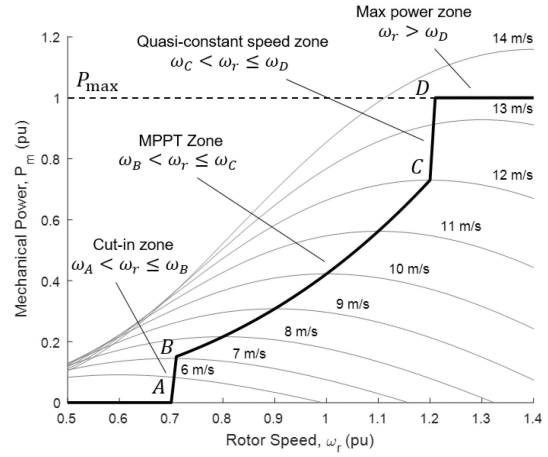


Fig. 1 WTG power point tracking [12]

speed zone, the active power reference is given by the equation below:

$$P_{ref} = \frac{(P_{max} - K_{opt} \omega_C^3)}{\omega_D - \omega_C} (\omega_r - \omega_C) + P_{max} \quad (6)$$

3.2.4 Zone 4: maximum power zone: For rotor speeds greater than ω_D , blade pitching is used to limit the active power reference to $P_{ref} = P_{max}$. Blade pitching reduces the power coefficient C_p , which reduces the amount of mechanical power that can be extracted from the available wind resource.

3.3 Emulated inertia and droop controllers

Fig. 2 shows a WTG frequency response system comprising emulated inertia and droop controllers based on [4]. The emulated inertia and droop controllers produce active power responses proportional to the RoCoF (RoCoF, df/dt) and frequency deviation (df), respectively. Under normal operating conditions, the power reference set point is determined by MPPT. Frequency disturbances, caused by load/generation imbalances, trigger active power responses from both controllers. The emulated inertia controller uses the time derivative of frequency to create the control signal ΔP_{in} that is inversely proportional to the RoCoF, thus negative RoCoF will cause ΔP_{in} to increase, while positive RoCoF will cause ΔP_{in} to decrease. The droop controller emulates the governor droop characteristic of a synchronous generator. Frequency deviation is measured and scaled by the droop constant $-K_d$ to produce the control signal ΔP_{droop} . Negative frequency deviation causes ΔP_{droop} to increase, while positive frequency deviation causes ΔP_{droop} to decrease. The control signal ΔP_{cont} is the summation of ΔP_{in} and ΔP_{droop} and emulates both the inertial and governor droop characteristics of a synchronous generator. The control signal ΔP_{cont} is added to P_{MPPT} to produce P_{ref} . When the WTG is operating in the MPPT zone of its power tracking characteristic (Fig. 1), the turbine is extracting maximum power from the available wind resource. The addition of positive ΔP_{cont} to P_{MPPT} means that the electromagnetic power supplied to the grid is greater than the mechanical power applied to the rotor shaft, which causes the rotor to decelerate. The increased active power output from the WTG acts to restore system frequency, thereby reducing the RoCoF and frequency deviation. Reduction in the RoCoF and frequency deviation reduces ΔP_{cont} . In addition to the reduction of ΔP_{cont} , as the rotor decelerates the active power set point from the MPP tracker P_{MPPT} also reduces.

The reduction in P_{MPPT} is due to rotor deceleration and means that the active power reference is only increased for a short duration; the duration being dependent on the magnitude of ΔP_{cont} , as the increased active power output decreases both P_{MPPT} and ΔP_{cont} . When the frequency is restored back to its nominal value, the active power reference is determined solely by MPPT.

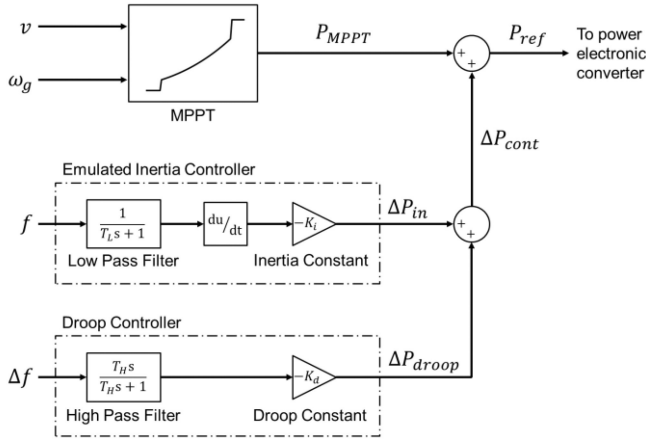


Fig. 2 Frequency response system based on [4]

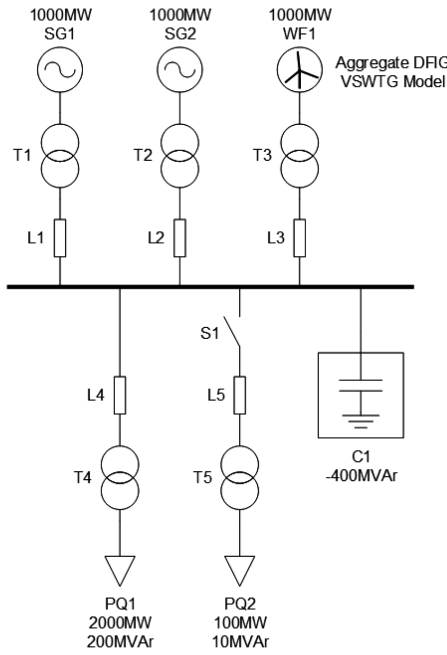


Fig. 3 MATLAB/Simulink Simscape power system model

However, after a period of increased active power output, the WTG operates at reduced, sub-optimal speed. A recovery period of reduced active power output is required to accelerate the rotor back to optimal speed, which can lead to a secondary frequency nadir while the power system is still in recovery from the initial frequency event [8].

3.4 Power system model

Fig. 3 shows the power system model used to evaluate different emulated inertia and droop controller designs. The model was built in MATLAB/Simulink using the Simscape Power Systems libraries and consists of two 1000 MW synchronous generators SG1 and SG2, a 1000 MW wind farm WF1, -400 MVar of power factor correction C1, and two loads PQ1 and PQ2. The synchronous generators SG1 and SG2 were configured as power voltage and swing-type generators, respectively. Both generators were modelled to employ AC1A excitation systems and steam turbine governors operating at 4% droop; this being the preferred governor droop setting for synchronous generators as specified in [13, 14]. The synchronous generator's active power reference settings were 0.8333 pu for SG1 and 0.8838 pu for SG2. An aggregate DFIG VSWTG model was used to model the wind farm. A constant wind speed of 10.8 m/s was used in all simulations. At this wind speed, the WTG was operating in the MPPT zone of its power tracking characteristic, producing an active power output of 0.518 pu. This equates to ~23% wind penetration. A small signal under-frequency

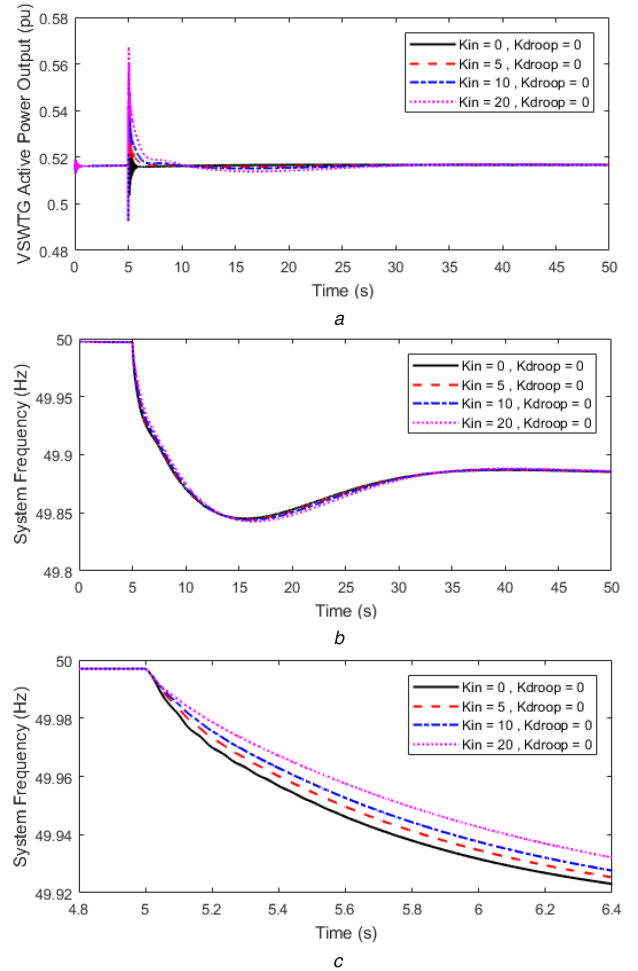


Fig. 4 Impact of emulated inertia controller

(a) VSWTG active power output, (b), (c) System frequency

event was simulated by connecting an additional 100 MW/10 MVar inductive load (PQ2) at $t = 5$ s.

4 Results and discussion

4.1 Emulated inertia controller: variation of K_{in}

Fig. 4 compares the VSWTG's active power output and the system frequency response to a sudden 5% increase in system load at $t = 5$ s. To investigate the emulated inertia controller's influence on system dynamics, the droop controller was deactivated by setting its droop constant to $K_{droop} = 0$, while the inertia constant K_{in} of the emulated inertia controller was varied from 0 to 20. Fig. 4a shows that the emulated inertia controller produces a very fast active power response to the grid imbalance; the magnitude of the response being proportional to K_{in} . This is an intuitive result as maximum RoCoF occurs at the inception of a frequency event. The fast-acting emulated inertial response reduces the initial RoCoF; the magnitude of the initial RoCoF decreasing as K_{in} increases, see Fig. 4c. Wind generation's ability to provide fast-acting active power response to limit RoCoF will become very important as system non-synchronous penetration (SNSP) levels increase. However, due to the WTG's contribution to frequency support ending before the system frequency reaches its nadir, the emulated inertial response has minimal impact on the frequency nadir. The frequency support provided by the emulated inertia controller lasted ~3–5 s.

An interesting characteristic of the emulated inertia controller is that as the frequency begins to recover, the RoCoF becomes positive, which results in ΔP_{in} becoming negative. This reduces the WTG's active power reference while the system is still in recovery, which results in a slightly reduced frequency nadir as K_{in} increases.

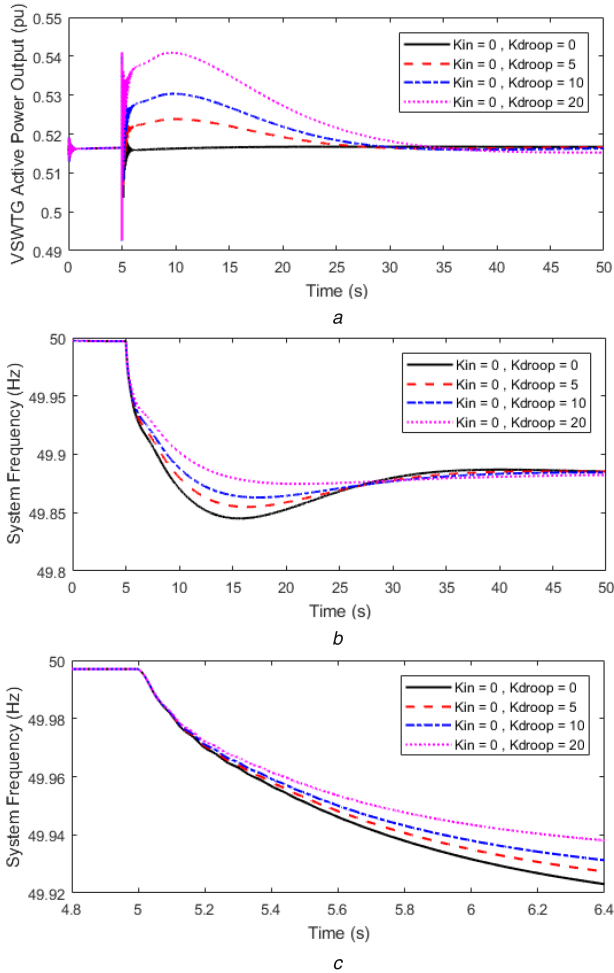


Fig. 5 Impact of droop controller
(a) VSWTG active power output, (b), (c) System frequency

4.2 Droop controller: variation in K_{droop}

Fig. 5 compares the VSWTG's active power output and the system frequency response to a sudden 5% increase in system load at $t = 5$ s. To investigate the droop controller's influence on system dynamics, the emulated inertia controller was deactivated by setting its inertia constant to $K_{in} = 0$, while the droop constant K_{droop} of the droop controller was varied from 0 to 20. Referring to Fig. 5a, the duration of the WTG's increased active power output is significantly longer than that produced by the emulated inertia controller; in the order of tens of seconds as opposed to seconds in the case of the emulated inertia controller. Under droop control, the WTG maintains an increased active power output for ~20–25 s. The problem with increasing the WTG's active power output is that it cannot be sustained for long periods without causing significant over-deceleration.

In theory, a large increase in active power output is desirable as it increases the frequency nadir. Fig. 5b shows that increasing K_{droop} significantly increases the frequency nadir, as increasing K_{droop} increases the magnitude of the WTG's active power response. Unfortunately, the increased frequency nadir comes at the expense of rotor speed. As the WTG expends more and more kinetic energy, the rotor decelerates further from optimal operating speed. The larger the increase in active power output, the further the rotor deviates from optimum speed. Hence, a longer recovery period is required to accelerate the rotor back to optimum speed. Fig. 5c shows that the variation of K_{droop} has no appreciable effect on the initial RoCoF.

The simulation results clearly show that the emulated inertia controller is more dominant than the droop controller in the initial few seconds after the inception of the frequency disturbance. However, its dominance reduces as the system frequency begins to recover and the magnitude of the RoCoF reduces. In contrast, the

droop controller has no appreciable effect on the initial RoCoF. As the system frequency deviates further from the nominal frequency, the droop controller's dominance increases, which helps to increase the frequency nadir.

5 Removing frequency support

The turbine and generator of a WTG have kinetic energy stored in their large rotating masses. It is this stored kinetic energy that is used to provide the increased active power output after an under-frequency event. When the WTG's active power output increases, its rotor slows down, as the electrical power generated and supplied to the grid is greater than the mechanical power delivered to the rotor. The difficulty with frequency response control schemes is that once the kinetic energy is used, it must be restored. The generator must supply reduced active power output for a period after the initial response to restore the expended kinetic energy. This restoration or recovery period allows the WTG's rotor to accelerate back to optimal operating speed. The kinetic energy required to accelerate the rotor from its post-frequency support speed to optimal operating speed is equal to the kinetic energy used during the frequency support. This can be estimated using the equation below:

$$E_{kinetic} = \frac{1}{2} J (\omega_{opt}^2 - \omega_1^2) \quad (7)$$

where $E_{kinetic}$ is the kinetic energy, J is the moment of inertia of the WTG, ω_{opt} is the optimum rotor speed, and ω_1 is the post-frequency support rotor speed. The time that it takes the rotor to accelerate to optimum speed is dependent on the magnitude of the active power reduction, hence a larger reduction in the WTG's active power output will require a shorter acceleration time. The difficulty with a large reduction in the WTG's active power output is that a lower secondary frequency nadir and increased RoCoF will ensue. Therefore, a compromise must be made between the duration of the acceleration phase and the system frequency response. The WTG's rotor can be accelerated by removing the frequency support (disconnecting the output of the emulated inertia and droop controllers). The sudden removal of the WTG's frequency support will cause a sudden drop in system frequency, due to the grid imbalance caused by the loss of generation. This results in a secondary frequency nadir. However, if the WTG's frequency support is gradually removed, the impact on system frequency can be minimised. Fig. 6 compares the system frequency response and VSWTG active power and rotor speed dynamics when the VSWTG's frequency support is removed according to the controller designs of Fig. 6a.

The results show that sudden removal of the WTG's frequency support at $t = 50$ s (Controller A) causes a significant secondary frequency nadir, which is lower than the frequency nadir of the system operating without frequency support from the WTG (base case). The magnitude of the secondary frequency dip is dependent on the magnitude of the frequency response system's controller output (ΔP_{cont}) at the time of its removal. A better solution is to gradually remove frequency support (Controller B). Controller B has a significantly lower impact on the system frequency. Gradual removal of the WTG's frequency support also results in smoother acceleration of the rotor back to optimum speed. Regardless of the frequency support removal strategy implemented, restoring the WTG's kinetic energy when the power system is still in recovery from the initial grid imbalance could lead to instability. Hence, to protect the power system against instability, the frequency support provided by WTGs should only be removed when the system is in steady state.

6 Conclusion

This paper has presented a review of WTG frequency response systems that allow WTGs to participate in grid balancing services by emulating the natural inertia and droop characteristics of conventional synchronous thermal generators. The MATLAB/Simulink simulation results show that emulated inertia controllers

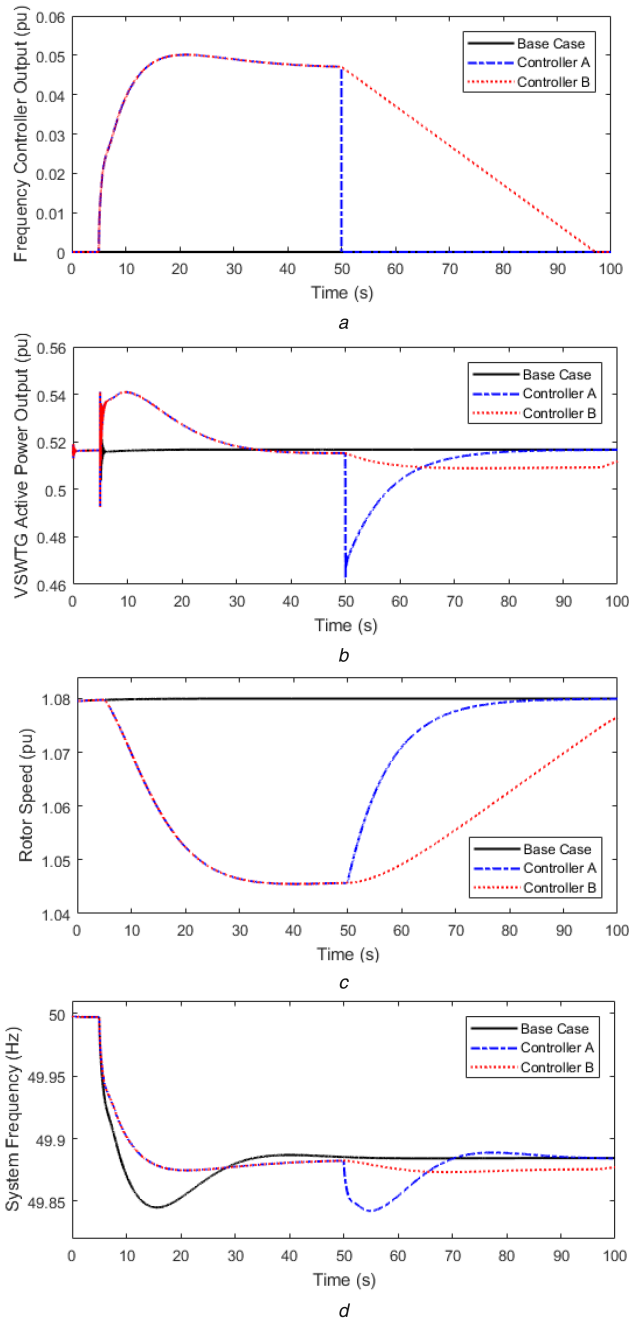


Fig. 6 Removal of frequency support

(a) Frequency response system controller output, (b) VSWG active power output, (c) VSWG rotor speed, (d) System frequency. Base case: no frequency support provided by the VSWG. Controller A: frequency support suddenly switched off at $t=50$ s. Controller B: frequency support gradually removed at $t=50$ s using a linear decline characteristic with a slew rate of -0.001 pu/s

can provide fast-acting active power responses to frequency events, which can reduce the magnitude of the RoCoF. The ability of

WTGs to provide fast-acting frequency support will become more important as the natural inertia of power systems reduce as SNSP levels increase. In contrast, the droop controller produced a slower active power response, proportional to frequency deviation. The droop controller maintained increased active power output for a longer duration than the emulated inertia controller; in the order of tens of seconds as opposed to seconds in the case of the emulated inertia controller. As a result, the droop controller was more dominant than the emulated inertia controller over the entirety of the frequency dynamic. Grid protection requires sustained and robust preservation, particularly with greater penetration of low-inertia generation. As SNSP levels increase, it will become essential for wind farms to provide controllable frequency response services to grid operators, to protect against frequency instability. However, increasing the WTG's active power output, in response to an under-frequency event, comes at the expense of rotor speed, and when operating under MPPT a recovery period of reduced active power output is required to accelerate the rotor back to optimal operating speed. The simulation results show that linearly decreasing the output of the emulated inertia and droop controllers reduces the impact that the VSWG's recovery period has on system frequency. The conclusion presented in this paper is that the implementation of emulated inertia and droop controllers will allow wind farms to provide grid balancing, AGC services, which can protect low-inertia power systems from frequency instability, whilst operating at high SNSP.

7 References

- [1] Kundur, P.: 'Power system stability and control' (McGraw-Hill, New York, 1994, 1st edn.)
- [2] Holdsworth, L., Ekanayake, J.B., Jenkins, N.: 'Power system frequency response from fixed speed and doubly fed induction generator-based wind turbines', *Wind Energy*, 2004, **7**, (1), pp. 21–35
- [3] Ackermann, T.: 'Wind power in power systems' (Wiley, Chichester, 2012, 2nd edn.)
- [4] Morren, J., de Haan, S.W., Kling, W.L., *et al.*: 'Wind turbines emulating inertia and supporting primary frequency control', *IEEE Trans. Power Syst.*, 2006, **21**, (1), pp. 433–434
- [5] Morren, J., Pierik, J., de Haan, S.W.: 'Inertial response of variable speed wind turbines', *Electr. Power Syst. Res.*, 2006, **76**, (11), pp. 980–987
- [6] Zhang, X., Wang, Y., Fu, Y., *et al.*: 'A novel method for obtaining virtual inertial response of DFIG-based wind turbines', *Wind Energy*, 2016, **19**, (2), pp. 313–328
- [7] Rutledge, L., Flynn, D.: 'Emulated inertial response from wind turbines: gain scheduling and resource coordination', *IEEE Trans. Power Syst.*, 2016, **31**, (5), pp. 3747–3755
- [8] Kang, M., Muljadi, E., Hur, K., *et al.*: 'Stable adaptive inertial control of a doubly-fed induction generator', *IEEE Trans. Smart Grid*, 2016, **7**, (6), pp. 2971–2979
- [9] Conroy, J., Watson, R.: 'Aggregate modelling of wind farms containing full-converter wind turbine generators with permanent magnet synchronous machines: transient stability studies', *IET Renew. Power Gener.*, 2009, **3**, (1), pp. 39–52
- [10] Heier, S.: 'Grid integration of wind energy conversion systems' (Wiley, Chichester, 2006, 2nd edn.)
- [11] Machowski, J., Bialek, J., Bumby, J.R.: 'Power system dynamics' (Wiley, Chichester, 2009, 2nd edn.)
- [12] Ochoa, D., Martinez, S.: 'Fast-frequency response provided by DFIG-wind turbines and its impact on the grid', *IEEE Trans. Power Syst.*, 2017, **32**, (5), pp. 4002–4011
- [13] EirGrid grid code version 6. Available at <http://www.eirgridgroup.com/site-files/library/EirGrid/GridCodeVersion6.pdf>, accessed 31 October 2017
- [14] SONI grid code. Available at <http://www.soni.ltd.uk/media/documents/Operations/Grid-Code/SONI%20Grid%20Code%20Version%20Aug%202015.pdf>, accessed 31 October 2017